Materials Research. 2019; 22(6): e20180306
DOI: http://dx.doi.org/10.1590/1980-5373-MR-2018-0306

Investigation of Physicochemical Characteristics of Heavy, Medium and Blend Crude Petroleum on Corrosion Resistance of AISI 1020 Carbon Steel

***Paula Cisquini*[a]*, *Simão Vervloet Ramos*[b], *Andrew Michael Tilley*[c], *Deise Menezes Santos*[d],**

***Vanessa de Freitas Cunha Lins*[a], *Marcos Benedito José Geraldo de Freitas*[d]**

[a]*Departamento de Engenharia Mecânica, Universidade Federal de Minhas Gerais – UFMG, Av. Antônio Carlos, 6627, CEP: 30270-901, Pampulha, MG, Brasil.*
[b]*Departamento de Engenharia Metalúrgica e de Materiais, Universidade Federal de Minhas Gerais – UFMG, Av. Antônio Carlos, 6627, CEP: 30270-901, Pampulha, MG, Brasil.*
[c]*Department of Chemical and Biomolecular Engineering, University of Connecticut, 191 Auditorium Road, Storrs, Connecticut, CT 06269-3222, United States.*
[d]*Laboratório de Pesquisa e Desenvolvimento de Metodologias para Análise de Petróleo (LABPETRO), Departamento de Química, Universidade Federal do Espírito Santo, Av. Fernando Ferrari 514, Goiabeiras, Vitória, ES, CEP: 29075-910, Brasil.*

Received: April 25, 2018; Revised: August 19, 2019; Accepted: October 24, 2019

This work investigates the influence of the physicochemical characteristics of heavy (17.5 °API), medium (28.3 °API) and blend (50% heavy + 50% medium) crude petroleum on corrosion of AISI 1020 carbon steel at 25.0 ± 1.0°C. The corrosion resistance of steel was analyzed by electrochemical impedance spectroscopy, potentiodynamic polarization, and scanning electron microscopy. The electrochemical results and the micrographs show that the corrosion on steel surfaces after contact with the heavy oil is lesser than medium and blend petroleum, although the heavy oil presents a higher amount of total acid number, sulfur compounds and salt. On steel sample immersed in heavy oil, a localized pitting corrosion was identified, while on samples immersed in medium and blend petroleum was found evidence of pitting and alveolar corrosion.

Keywords: *Crude petroleum, physicochemical characteristics, electrochemical impedance spectroscopy, potentiodynamic polarization, corrosion.*

1. Introduction

Petroleum is a mixture of hydrocarbons and compounds containing sulfur, nitrogen, oxygen and metals [1]. The American Petroleum Institute classifies petroleum by degrees (°API). Petroleum with °API less than 20 is classified as heavy, °API between 21-30 as medium, and °API greater than 30 as light. In heavier petroleum, there are high proportions of aromatics, resins, asphaltenes and sulfur compounds [2]. The high concentration of resins and asphaltenes increases the density and, consequently, the viscosity of petroleum [3]. In lighter petroleum, there are high proportions of the paraffinic and naphthenic acids, and a lower concentration of the sulfur compounds. Light and medium oils have a higher market value, because of the derivatives, such as naphtha, gasoline and diesel, which are more valuable. Therefore, the blend of different types of oils has been carried out by petroleum industry to obtain added value.

In the oil and gas industry, the carbon steels are still the most used alloys. Carbon steels has low cost, good weldability and adequate mechanical strength for most applications in the petrochemical industry, however has low corrosion resistance in several media [4]. Therefore, the knowledge about the corrosion behavior of this steel in contact with different types of petroleum and its interaction can provide valuable information of corrosive agents for each oil.

The main causes of corrosion by petroleum are the naphthenic acids, H_2S, oxygen, amines, cyanides, sulfur compounds, hydrogen gas and salt [5]. Among those, naphthenic acids are one of the foremost corrosive agents of petroleum. Deyab et al. [6] verified that corrosion in carbon steel increased as a function of the molar weight of naphthenic acid, reaching a maximum value for acid species with a carbon number equal to 9 (C9), after that the corrosion rate decreased. The presence of salt in petroleum also makes the carbon steel susceptible to corrosion. Veloz and Gonzalez [7] identified that the chlorides control the corrosion process and may inhibit passive film formation on carbon steel when immersed in solution containing chlorides and H_2S.

The thermodynamics of hydrogen sulfide and iron-sulfide systems it is also important to understand [8,9]. In the presence of sulfur compounds, many types of iron sulfides may form as corrosion products in carbon steels, such as mackinawite ($Fe_{1+x}S$), cubic ferrous sulfide (FeS), smythite ($Fe_{3+x}S_4$), greigite (Fe_3S_4), pyrrhotite ($Fe_{1-x}S$), troilite (FeS), and pyrite (FeS_2), which have different crystal structures, oxidation states, and Fe-S stoichiometry [10,11]. These films are formed on metal surfaces due to the adsorption of compounds containing sulfur, nitrogen and oxygen. However, the corrosion product formed by oxidation of steel and alloys may or may not have protective properties [8,12,13]. For example, mackinawite layer is porous, has no passivating properties and allows the dissolution of the steel.

*e-mail: paulacisquini@gmail.com

Besides the elements mentioned above, petroleum also contains resins and asphaltenes that aggregate in the form of colloids [14] and block the mobility of the ionic species [3]. Therefore, petroleum consists in a complex system with different compounds acting simultaneously, such as highly corrosive impurities, ionic mobility blockers and non-corrosive compounds.

Electrochemical techniques can be used in situ and are great options for crude-oil environment. In this work, aided by electrochemical techniques and scanning electron microscopy, the corrosion of AISI 1020 carbon steel immersed in heavy (17.5 °API), medium (28.3 °API) and blend (50% heavy + 50% medium) crude petroleum was studied. Aiming to study the influence of physicochemical characteristics on the corrosion, samples of heavy oil (more viscous) with a greater amount of salt content, total acid number and sulfur compounds were selected, as well as medium oil (less viscous), with less concentration of the corrosive agents. From electrochemical impedance spectroscopy and potentiodynamic polarization measurements, electrochemical parameters of petroleum and emulsions of water-in-oil type were obtained, such as conductivity, capacitance and polarization resistance.

2. Experimental

2.1 Petroleum characterization

In this work, samples of petroleum from the same field, but different reservoirs located in Espírito Santo-Brazil, were used. Table 1 shows the characterization of physicochemical properties of the petroleum samples in natura. In the oil characterization process, initially the free water was separated by decanting for an hour. After decanting, the analysis of Bottom Sediment Water (BSW) (D 4007-08)[15] was carried out to evaluate the content of the water and sediment in the petroleum. In the demulsification process, 50 mL of emulsioned oil was dehydrated with the addition of 0.25 µL of the concentrated demulsifier, heated at 80°C for 20 minutes and centrifuged at 2000 rpm for 10 minutes.

Table 1. Characterization of the heavy and medium petroleum samples.

Petroleum Characterization	Heavy	Medium
Salt content (ppm)	13.533	10.210
Sulfur Content (% m/m)	0.5432	0.1567
Number of Total Acid (mg KOH/g^{-1})	3.1651	0.4249
Oil Density at 20/4°C (g/cm^3)	0.9455	0.8820
API Degree at 60 °F	17.5	28.3
Viscosity 20°C (cSt)	562.95	80.86
Viscosity 40°C (cSt)	441.50	27.02
Viscosity 50°C (cSt)	253.95	18.39
Pour Point (°C)	-21.0	-12.0
Bottom Sediment Water (% v/v)	7.00	7.00

After demulsification, the BSW was again determined in this stage to verify if the water and sediment content were lower than 0.5% v/v. The physicochemical properties of dehydrated petroleum, such as salt content (ASTM D 6470-99)[16], sulfur content (ASTM D 4294 – 10)[17], total acid numbers (ASTM D 664-09)[18], density (ASTM D 5002-99)[19], API degree (ASTM D1298-99)[20], cinematic viscosity (ASTM D 7042 -04)[21], and pour point (ASTM D 97-04)[22] were determined, Table 1.

2.2 Electrochemical measurements

A two-electrode cell was used due to the high impedance of the petroleum. This arrangement has been used in petroleum analysis [23,24]. Similar conditions are commonly used to analyze ceramic materials and polymers. The electrochemical cell consists of a counter electrode (CE) of platinum with total area of 3.5 cm^2 and the working electrode (WE) of AISI 1020 steel with total area between 0.20 cm^2 and 0.28 cm^2, attached to a beaker (10.0 mL) and Teflon cap. The distance between electrodes was 0.55 mm. For the surface preparation, the working electrode was polished with sandpaper of #80, #120, #320, #400 and #600 grits, washed out with distilled water, and then hot-dried. The oil samples were homogenized for 5 minutes on the shaker Turrax T25 (9500 RPM). Before each measurement, the electrodes were washed out with ethanol and acetone in ultrasound bath. The electrodes were hot-dried and immediately inserted into the electrochemical cell, and the reference electrode was connected to a counter electrode.

The electrochemical techniques used were open circuit potential, electrochemical impedance spectroscopy (EIS) and potentiodynamic polarization. The potential and current in the open circuit were measured for 24 hours and obtained constant values for each oil. To carry out the impedance measurements, the system followed the principles of linearity, stationarity and causality, and was validated by Kramers-Kronig transforms. The EIS measurements were performed in the frequency range 10.0 kHz – 1.0 mHz, ten points per decade, with an amplitude of ± 350 mV DC. Potentiodynamic measurements were performed from the open circuit potential until 1.5 V vs Pt at a scan rate of 10 mVs^{-1}. A potentiostat/galvanostat Autolab PGSTAT 100 ECHO CHIMIE was used with an ECD module for low currents (in the order of pA) and a Faraday cage was used to minimize the noise. The experiments were conducted at temperatures of 25.0 ± 1.0°C. In order to ensure statistical relevance, triplicates of each experiment were performed. After the electrochemical tests, the steel samples were cleaned with kerosene to remove oil, then pickling was carried out with Clark solution (1L HCl + 20g Sb_2O_3 + 50g $SnCl_2$) for 5 seconds, aiming to dissolve the corrosion products, and then washed with distilled water, hot-dried and stored in a desiccator. The surface analyses of AISI 1020 steel after corrosion tests were performed by scanning electron microscopy (SEM) with 120 kV and 21 mm working distance using the JSM 6610 LV.

3. Results and Discussion

3.1 Electrochemical impedance spectroscopy and potentiodynamic polarization

Figure 1 shows the electrochemical impedance spectroscopy (EIS) measurements for heavy (17.5 °API), medium (28.3 °API) and blends (50% heavy + 50% medium) crude petroleum. Using the EIS technique, it is possible to analyze different processes that occur in volume phase, and at the electrode/oil interface, in the same measurement.

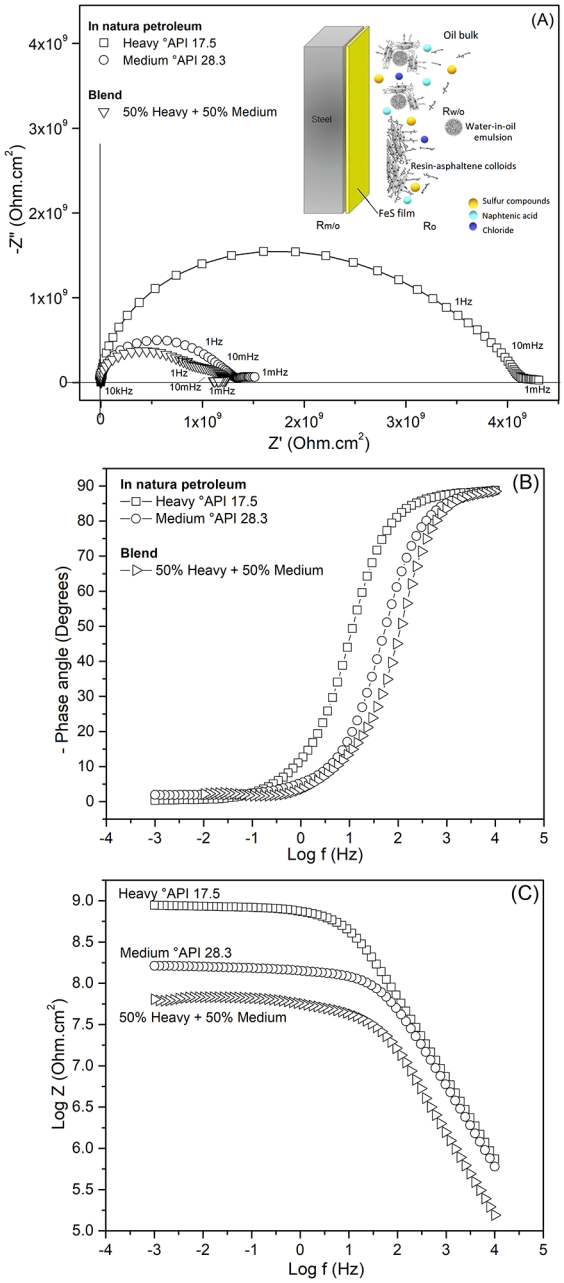

Figure 1. Nyquist diagram (A) and Bode diagram: phase angle (B) and impedance module (C). Potential amplitude of ± 350 mV, frequency interval 10.0 kHz - 1.0 mHz.

The Nyquist diagram (Figure 1A) shows the real component (Z') and the imaginary component (-Z'') of impedance of the AISI 1020 steel in contact with different oils and their blend. The AISI 1020 steel immersed in heavy petroleum presented larger semicircle diameter than medium and blend petroleum, which indicates a higher polarization resistance due to a high charge transfer resistance. The steel in contact with the blend petroleum resulted in the smallest polarization resistance indicating a higher conductivity. Blend semicircles also presented a resistance reduction in low-frequency region probably indicating a corrosive process on metal surface. This behavior was not observed in the curves of the medium and heavy petroleum samples.

The Bode diagram is represented by the phase angle (θ) (Figure 1B) and impedance module (IZI) (Figure 1C), both as a function of the frequency. In the regions of high (10 kHz – 1.0 Hz) and medium (1.0 Hz – 10 mHz) frequencies were analyzed processes that occurs in the petroleum volume phase such as diffusion. In the region of low frequency (10 mHz – 1.0 mHz) it was analyzed processes that occur at the metal/oil interface, such as charge transfer reactions, adsorption and desorption of organic compounds and metal corrosion.

The phase angle curves of all petroleum samples (Figure 1B) varies from 0° to -90° due to an ideal capacitor behavior. For the heavy oil, the phase angle curve was more shifted to medium frequencies regions and the impedance module (Figure 1C) was higher than medium and blend petroleum, due to its higher resistivity. For the blend sample, the impedance modulus (Figure 1C) was lower than in medium and heavy petroleum. These results show that the blending of the oils with different API degree leaded to a reduction of the polarization resistance to lower values than the reference oils values, when applied a potential amplitude of ± 350 mV.

Although homogeneous distribution of the time constant in the Nyquist and Bode diagrams, there are different contributions in the system, which can be seen in the simulated equivalent circuit (Figure 2). The equivalent circuit for all petroleum samples was $(R_oC_o)(R_{w/o}Q_{w/o})(R_{m/o}Q_{m/o})$, where Ro and Co are the polarization resistance and capacitance in the volume phase of oil, $R_{w/o}$ and $Q_{w/o}$ represent the water-in-oil emulsions, Rm/o is the polarization resistance of the metal-oil interface that can be correlated with metal corrosion and $Q_{m/o}$ is the constant phase element for heterogeneity of the interface metal/oil. All simulations had a chi-squared lower than 10^{-4}.

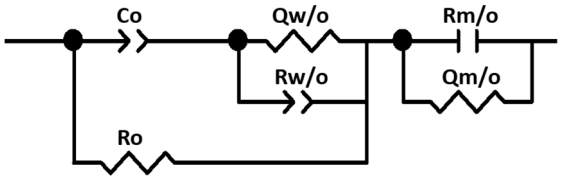

Figure 2. Equivalent circuit for AISI 1020 steel in heavy, medium and blend crude petroleum.

The individual contributions of the different polarization resistance in all systems are listed in Table 2. The resistance of the oil volume phase (R_o), water-in-oil emulsion ($R_{w/o}$) and metal/oil interface ($R_{m/o}$) increases with the decreasing of API degree.

In the heavy oil sample, salt content, total acid number (TAN) and sulfur compounds are greater than medium petroleum samples, as shown in Table 1. It was expected that polarization resistance (R_o) for volume phase of heavy petroleum would decrease due to the amount of polar and ionic compounds are greater than in the medium oil sample, Table 2. However, this behavior was not observed. It can be explained by the presence of greater amounts of resins and asphaltenes that increases the density and consequently, the viscosity of heavy petroleum [3]. Aggregates are formed in the volume phase of heavy oil by resins bonded to asphaltene cores by polar functional group interactions [14], schematically illustrated in Figure 1A. As a result, resin-asphaltene aggregates can act as a blocking agent in the volume phase of petroleum decreasing the ion mobility. In the case of blend sample, mixing heavy and medium oils reduces the concentration of resins and asphaltenes, decreasing the density and viscosity which leads to increase diffusion of the corrosive species. The relationship between resistance, ionic concentration and mobility is given in Equation 1:

$$R = \frac{l}{Ak} = \frac{l}{AF\sum_i^j zC\mu} \qquad \text{(Eq. 1)}$$

Where "k" is conductivity, "F" is Faraday constant, "μ" is ionic mobility of the compound, "z" is charge of the compound, and "C" is concentration of the compound.

The volume phase capacitance (C_o) for heavy oil is higher than for medium and blend (Table 2) due to an increase in the dielectric constant (ε) when A/l ratio is constant. This demonstrates that the structure of the polar components in the heavy petroleum is less organized. The capacitance is given by Equation 2.

$$C = \varepsilon\frac{A}{l} \qquad \text{(Eq. 2)}$$

Where "ε" is dielectric constant, "A" is area and "l" is length.

The high polarization resistance of water-in-oil emulsion ($R_{w/o}$), and consequently, the lower value of constant phase element of water-in-oil emulsion ($Q_{w/o}$) for the heavy petroleum sample, Table 2, occurred due to the high concentration of resins and asphaltenes. The interactions between asphaltene and resin molecules and their association form an interfacial film on water-in-oil emulsions (see in Figure 1A), promoting its stabilization [25]. The n values indicate the deviation of the constant phase element (Q) from a pure capacitance, in which n value equal to 1 characterizes an ideal capacitor.

The high polarization resistance at the metal/oil interface ($R_{m/o}$) for heavy petroleum, may indicate the formation of a passive film on the steel surface. According to literature [8,26], a greater amount of sulfur compounds in heavy oil may lead to passive ferrous sulfide (FeS) films production. In the case of low concentrations of sulfur compounds, a non-passivating porous film such as mackinawite (Fe_1+Xs) may be produced [10], which possibly occurred in medium and blend petroleum. In the metal/oil interface of the blend, a lower polarization resistance ($R_{m/o}$) and a higher constant phase element ($Q_{m/o}$) associated to the lesser $n_{m/o}$ value, probably indicate a corrosive process on steel surface. This can be explained by its higher conductivity in oil volume phase and the formation of a non-protective film.

Figure 3 shows the potentiodynamic polarization curves obtained up to an anodic potential of +1.50 $V_{(SCE)}$ in AISI 1020 steel immersed in petroleum with different API degree and its blend. The potentiodynamic measurements provide parameters such as current density, resistance and overpotential of the whole system, composed of the electrode and petroleum. It is not possible to separate the contributions of the interface electrode/oil and the volume phase, due to the high ohmic petroleum resistance.

In the voltammograms (Figure 3), the current density values for blend sample (50% heavy + 50% medium) are in between those of heavy (17.5 °API) and medium (28.3 °API) crude petroleum. The values of resistance (R), calculated from the potentiodynamic polarization (Eq. 3), for heavy, medium and blend oils, are respectively 0.84 GΩ.cm^2, 0.17 GΩ.cm^2 and 0.24 GΩ.cm^2 (Table 3). The blend oil behavior was different from EIS analysis (Figure 1), where it presented a lower polarization resistance than their reference oils, when applied a potential amplitude of ± 350 mV.

Table 2. Simulation values of equivalent circuit for AISI 1020 steel in heavy, medium and blend petroleum.

Oil	R_o GOhm.cm^2	C_o pF.cm^{-2}	$R_{w/o}$ GOhm.cm^2	$Q_{w/o}$ Ohm^{-1}.cm^{-2}.s^n	$n_{w/o}$	$R_{m/o}$ GOhm.cm^2	$Q_{m/o}$ Ohm^{-1}.cm^{-2}.s^n	$n_{m/o}$	Chi-Squared
Heavy	1.42	0.023	2.22	0.067	0.92	4.06	0.009	0.97	9.8x10^{-5}
Error (%)	4.6	10.1	2.7	7.4	3.2	15.5	2.2	0.98	---
Medium	0.59	0.007	0.55	1.000	0.81	1.22	0.073	0.92	1.4x10^{-4}
Error (%)	2.7	2.0	2.5	12.6	7.95	15.7	9.3	2.90	--
Blend	0.31	0.008	0.27	0.099	0.90	0.42	1.52	0.69	5.6x10^{-4}
Error (%)	3.9	10.4	2.1	7.8	2.3	9.4	3.6	0.84	---

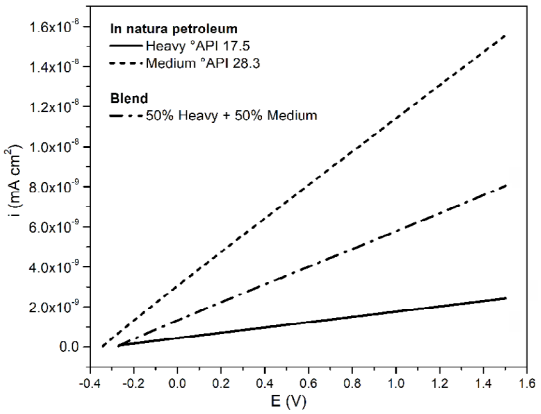

Figure 3. Potentiodynamic polarization of AISI 1020 steel immersed in heavy, medium and blend petroleum, rate scan of 10 mVs^{-1}.

Table 3. Conductance (G), resistance (R) and conductivity (k) calculated from the potentiodynamic polarization for AISI 1020 steel in heavy, medium and blend petroleum.

Oil	G (nS)	R (GOhm.cm²)	k (nS.cm-¹)
Heavy	0.10	0.84	0.03
Medium	0.50	0.17	0.20
Blend	0.40	0.24	0.09

The potentiodynamic polarization results show that the blend resistance is changed when subjected to a more positive potential (+1.50 $V_{(SCE)}$) probably occurring due to the high charge transfer resistance of the asphaltenes and resins that act as ionic blockers in volume phase of oil.

The resistance (R) is given below in Equation 3:

$$R = \frac{di}{dE} \qquad \text{(Eq. 3)}$$

Where "i" is current and E is potential.

3.2 Surface characterization of AISI 1020 steel, after electrochemical impedance spectroscopy and potentiodynamic polarization measurement

Figure 4 shows the surface micrographs of AISI 1020 steel after electrochemical impedance spectroscopy and potentiodynamic polarization analyses in heavy (17.5 °API), medium (28.3 °API) and blend (50% heavy + 50% medium) crude petroleum. On untested sample (Figure 4A) corrosive processes were not observed on the surface. There were only grooves caused by mechanical polishing during the surface preparation.

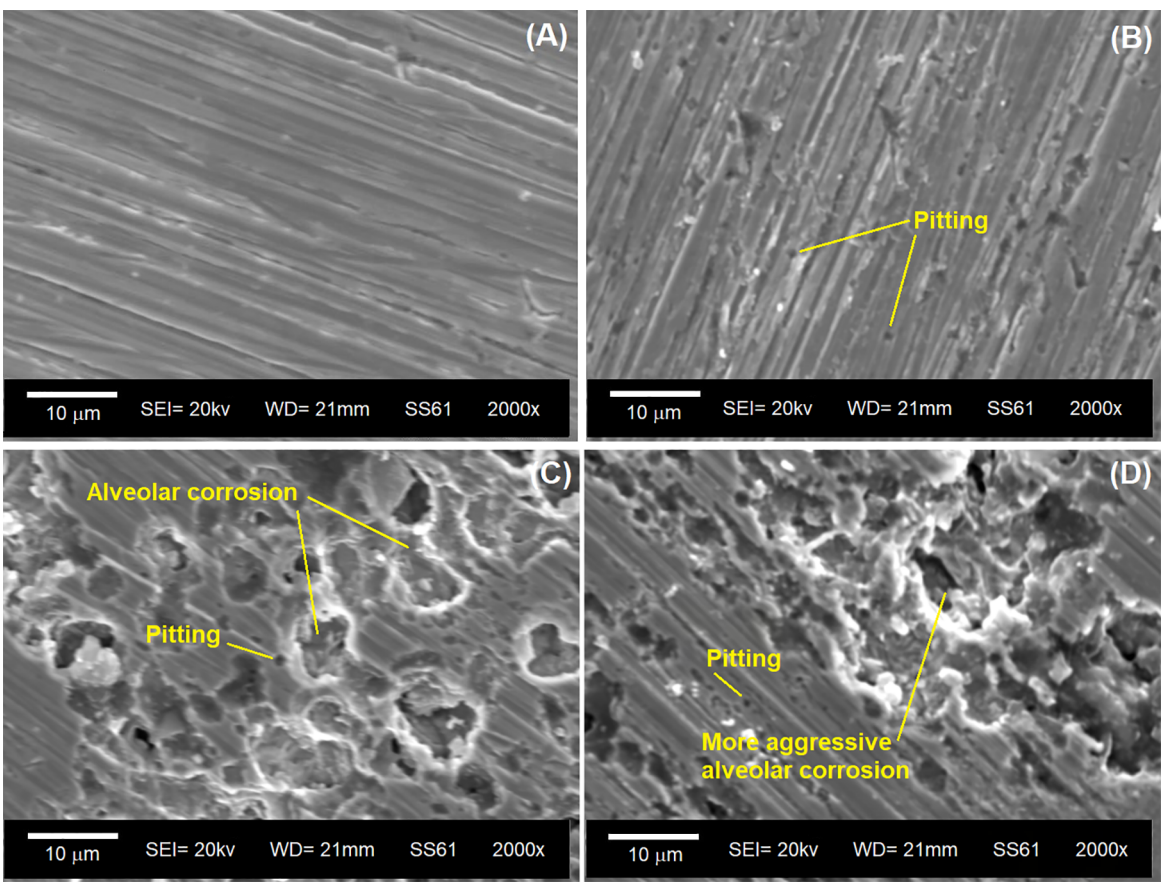

Figure 4. SEM micrographs of the AISI 1020 steel (A) untested sample and immersed in (B) heavy, (C) medium and (D) blend petroleum.

On the AISI 1020 steel after contact with the heavy petroleum (Figure 4B) there was only localized corrosion by pitting. The resin-asphaltene colloids in heavy petroleum act as ionic mobility blockers [3,14] acting as natural inhibitors of the corrosion process. Besides that, the greater amount of sulfur compounds in heavy oil may produce passive ferrous sulfide films (FeS) on steel surface [8,26], which inhibits the naphthenic corrosion [27,28] and decreases the chloride corrosion [24]. The surface micrographs confirmed the electrochemical results previously shown in Figures 1 and 3.

On the sample immersed in medium petroleum (Figure 4C), the surface morphology of the corroded areas revealed pitting and alveolar corrosion. This occurs due to the medium petroleum has a lower viscosity allowing the ion mobility of corrosive agents, and its lower concentrations of sulfur compounds produce a porous film that allows the dissolution of the metal[10].

On the sample exposed to the blend (50% Heavy + 50% Medium) (Figure 4D), the pitting and alveolar corrosion were more aggressive than in medium and heavy oil. This severe corrosion can be explained by the convergence of different factors, in which the lower viscosity of the medium oil gave mobility to high amounts of corrosive agents of heavy oil.

The electrochemical analyses of petroleum with different API degrees and its blend confirm that the petroleum is a complex system that has a number of factors which simultaneously accelerate and retard corrosion processes. The results show that at temperature of 25.0 ± 1.0°C the viscosity had greater influence on the corrosion than the concentration of corrosive agents. This reveals that the acidity content is not enough to determine the petroleum corrosivity [29]. Therefore, for corrosion analyses, it is important to consider the concentration of corrosive agents [5]; thermodynamics of hydrogen sulfide and iron-sulfide systems [8,9]; as well as the temperature of the process [4,30] which directly influences on petroleum viscosity

4. Conclusions

Heavy (17.5 °API), medium (28.3 °API) and blend (50% heavy + 50% medium) crude petroleum were electrochemically studied to seek a correlation between physicochemical characteristics and corrosion process on AISI 1020 steel.

- The electrochemical impedance spectroscopy technique allows to interpret the phenomena that occurs in the volume phase and electrode interface. The equivalent circuit simulated for all petroleum samples is $(R_oC_o)(R_{w/o}Q_{w/o})(R_{m/o}Q_{m/o})$, where R_oC_o are the resistance and capacitance of the oil volume phase, $R_{w/o}$ and $Q_{w/o}$ represents the resistance and constant phase element of water-in-oil emulsions, $R_{m/o}$ is the polarization resistance of the metal-oil interface that can be correlated with metal corrosion and $Q_{m/o}$ is the constant phase element for the heterogeneity of the interface metal/oil. Heavy petroleum (4.06 GOhm.cm^2) presents a higher polarization resistance on metal-oil interface than medium petroleum (1.22 GOhm.cm^2) and their blend (0.42 GOhm.cm^2).
- In heavy petroleum, the high viscosity retards the charge carriers mobility inhibiting the pitting corrosion attack on steel surface. Medium petroleum despite possesses a lower concentration of corrosive agents; the species diffusion is facilitated by low viscosity and the corrosion takes place by pitting and alveolar. The blend of 50% heavy and 50% medium petroleum reduces the concentration of resins and asphaltenes and increases the diffusion of the corrosive species leading to an aggressive attack of pitting and alveolar corrosion.
- The acidity is not enough to determine the corrosivity of oils. For corrosion analyses, besides consider the corrosive elements and understanding of the thermodynamics of hydrogen sulfide and iron sulfide systems, it is important to consider the oil viscosity that influences in ionic mobility of the corrosive species.

5. Acknowledgements

The authors acknowledge PETROBRAS and the Brazilian research funding agencies CAPES and CNPq for their financial support.

6. References

1. McCain WD. *The Properties of Petroleum Fluids*. 3rd ed. Tulsa: PennWell; 2017.

2. Speight JG. *Heavy Oil Recovery and Upgrading*. Cambridge: Elsevier; 2019. DOI: 10.1016/C2016-0-04682-X

3. Sun H, Lei X, Shen B, Zhang H, Liu J, Li G, et al. Rheological properties and viscosity reduction of South China Sea crude oil. *Journal of Energy Chemistry*. 2018;27(4):1198-1207.

4. Heidersbach R. *Metallurgy and Corrosion Control in Oil and Gas Production*. Hoboken: John Wiley & Sons; 2018.

5. Groysman A. *Corrosion Problems and Solutions in Oil Refining and Petrochemical Industry*. Volume 61. 1st ed. Cham: Springer; 2017.

6. Deyab MA, Dief HAA, Eissa EA, Taman AR. Electrochemical investigations of naphthenic acid corrosion for carbon steel and the inhibitive effect by some ethoxylated fatty acids. *Electrochimica Acta*. 2007;52(28):8105-8110. DOI: 10.1016/j.electacta.2007.07.009

7. Veloz MA, González I. Electrochemical study of carbon steel corrosion in buffered acetic acid solutions with chlorides and H_2S. *Electrochimica Acta*. 2002;48(2):135-144. DOI: 10.1016/S0013-4686(02)00549-2

8. Wen X, Bai P, Luo B, Zheng S, Chen C. Review of recent progress in the study of corrosion products of steels in a hydrogen sulphide environment. *Corrosion Science*. 2018;139:124-140. DOI: 10.1016/j.corsci.2018.05.002

9. Ning J, Zheng Y, Young D, Brown B, Nešić S. Thermodynamic Study of Hydrogen Sulfide Corrosion of Mild Steel. *Corrosion*. 2013;70(4):375-389. DOI: 10.5006/0951

10. Perini N, Corradini PG, Nascimento VP, Passamani EC, Freitas MBJG. Characterization of AISI 1005 corrosion films grown under cyclic voltammetry of low sulfide ion concentrations. *Corrosion Science*. 2013;74:214-222. DOI: 10.1016/j.corsci.2013.04.045

11. Shi F, Zhang L, Yang J, Lu M, Ding J, Li H. Polymorphous FeS corrosion products of pipeline steel under highly sour conditions. *Corrosion Science*. 2016;102:103-113. DOI: 10.1016/j.corsci.2015.09.024

12. Tamura H. The role of rusts in corrosion and corrosion protection of iron and steel. *Corrosion Science*. 2008;50(7):1872-1883. DOI: 10.1016/j.corsci.2008.03.008

13. Panossian Z, de Almeida NL, de Sousa RMF, Pimenta GS, Marques LBS. Corrosion of carbon steel pipes and tanks by concentrated sulfuric acid: A review. *Corrosion Science*. 2012;58:1-11. DOI: 10.1016/j.corsci.2012.01.025

14. Sullivan AP, Kilpatrick PK. The Effects of Inorganic Solid Particles on Water and Crude Oil Emulsion Stability. *Industrial & Engineering Chemistry Research*. 2002;41(14):3389-3404. DOI: 10.1021/ie010927n

15. ASTM International. *ASTM D4007 - 08 - Standard Test Method for Water and Sediment in Crude Oil by the Centrifuge Method (Laboratory Procedure)*. West Conshohocken: ASTM International; 2008.

16. ASTM International. *ASTM D6470 - 99(2015) - Standard Test Method for Salt in Crude Oils (Potentiometric Method)*. West Conshohocken: ASTM International; 2015.

17. ASTM International. *ASTM D4294 - 16e1 - Standard Test Method for Sulfur in Petroleum and Petroleum Products by Energy Dispersive X-ray Fluorescence Spectrometry*. West Conshohocken: ASTM International; 2016.

18. ASTM International. *ASTM D664 - 09 - Standard Test Method for Acid Number of Petroleum Products by Potentiometric Titration*. West Conshohocken: ASTM International; 2009.

19. ASTM International. *ASTM D5002 - 99 - Standard Test Method for Density and Relative Density of Crude Oils by Digital Density Analyzer*. West Conshohocken: ASTM International; 1999.

20. ASTM International. A*STM D1298 - 99 - Standard Test Method for Density, Relative Density (Specific Gravity), or API Gravity of Crude Petroleum and Liquid Petroleum Products by Hydrometer Method*. West Conshohocken: ASTM International; 1999.

21. ASTM International. *ASTM D7042 - 04 - Standard Test Method for Dynamic Viscosity and Density of Liquids by Stabinger Viscometer (and the Calculation of Kinematic Viscosity)*. West Conshohocken: ASTM International; 2004.

22. ASTM International. *ASTM D97 - 04 - Standard Test Method for Pour Point of Petroleum Products*. West Conshohocken: ASTM International; 2004.

23. Perini N, Prado AR, Sad CMS, Castro EVR, Freitas MBJG. Electrochemical impedance spectroscopy for *in situ* petroleum analysis and water-in-oil emulsion characterization. *Fuel*. 2012;91(1):224-228. DOI: 10.1016/j.fuel.2011.06.057

24. Freitas S, Malacarne MM, Romão W, Dalmaschio GP, Castro EVR, Celante VG, et al. Analysis of the heavy oil distillation cuts corrosion by electrospray ionization FT-ICR mass spectrometry, electrochemical impedance spectroscopy, and scanning electron microscopy. *Fuel*. 2013;104:656-663. DOI: 10.1016/j.fuel.2012.05.003

25. da Silva M, Sad CMS, Pereira LB, Corona RRB, Bassane JFP, dos Santos FD, et al. Study of the stability and homogeneity of water in oil emulsions of heavy oil. *Fuel*. 2018;226:278-285. DOI: 10.1016/j.fuel.2018.04.011

26. Okonkwo PC, Sliem MH, Shakoor RA, Mohamed AMA, Abdullah AM. Effect of Temperature on the Corrosion Behavior of API X120 Pipeline Steel in H_2S Environment. *Journal of Materials Engineering and Performance*. 2017;26(8):3775-3783. DOI: 10.1007/s11665-017-2834-0

27. Yépez O. Influence of different sulfur compounds on corrosion due to naphthenic acid. *Fuel*. 2005;84(1):97-104. DOI: 10.1016/j.fuel.2004.08.003

28. Barros EV, Dias HP, Gomes AO, Rodrigues RRT, Moura RR, Sad CMS, et al. Study of degradation of acid crude oil by high resolution analytical techniques. *Journal of Petroleum Science and Engineering*. 2017;154:194-203. DOI: 10.1016/j.petrol.2017.04.032

29. Zeinalov EB, Abbasov VM, Alieva LI. Petroleum acids and corrosion. *Petroleum Chemistry*. 2009;49(3):185-192. DOI: 10.1134/S0965544109030013

30. Gao S, Brown B, Young D, Singer M. Formation of iron oxide and iron sulfide at high temperature and their effects on corrosion. *Corrosion Science*. 2018;135:167-176. DOI: 10.1016/j.corsci.2018.02.045